



Title	Refinement of As-cast Austenite Grain in Carbon Steel by Addition of Titanium
Author(s)	Sasaki, Masayoshi; Matsuura, Kiyotaka; Ohsasa, Kenichi; Ohno, Munekazu
Citation	ISIJ International, 49(9), 1362-1366 <a href="https://doi.org/10.2355/isijinternational.49.1362">https://doi.org/10.2355/isijinternational.49.1362</a>
Issue Date	2009-09-15
Doc URL	<a href="http://hdl.handle.net/2115/75411">http://hdl.handle.net/2115/75411</a>
Rights	著作権は日本鉄鋼協会にある
Type	article
File Information	ISIJ Int. 49(9)_ 1362-1366 (2009).pdf



[Instructions for use](#)

# Refinement of As-cast Austenite Grain in Carbon Steel by Addition of Titanium

Masayoshi SASAKI,<sup>1)</sup> Kiyotaka MATSUURA,<sup>2)</sup> Kenichi OHSASA<sup>2)</sup> and Munekazu OHNO<sup>2)</sup>

1) Formerly Graduate Student, Hokkaido University. Now at Sumitomo Metal Industries, Ltd., Minato, Wakayama, 640-8555 Japan.

2) Division of Materials Science and Engineering, Graduate School of Engineering, Hokkaido University, Kita 13 Nishi 8, Kita-ku, Sapporo 060-8628 Japan.

(Received on February 18, 2009; accepted on April 30, 2009; originally published in *Tetsu-to-Hagané*, Vol. 94, 2008, No. 11, pp. 491–495)

Effects of Ti addition on as-cast austenite structure of S45C steel have been investigated by means of furnace cooling experiment at a cooling rate of 0.03°C/s, focusing on the Ti addition ranging from 0 to 0.5 mol%. The Ti addition reduces average austenite grain diameter down to a size comparable to secondary dendrite arm spacing. In samples with the Ti addition, the austenite grain boundary is located at interdendritic position where Ti(C,N) particles exist and the refinement of austenite grain structure is ascribable to pinning effect of the Ti(C,N) particle formed in L+ $\gamma$ -Fe+Ti(C,N) phase field. The increment of Ti addition does not substantially change the size of Ti(C,N) particle but increases the number of the Ti(C,N) particles, leading to further refinement of the austenite grains.

KEY WORDS: carbon steel; solidification; peritectic reaction; austenite grain; grain refinement; inclusion; titanium carbonitride.

## 1. Introduction

Continuous casting process of carbon steel involves the formation of coarse as-cast austenite grain structure and the  $\gamma$  grain size often reaches several mm in size. Such a coarse  $\gamma$  grain structure causes surface cracking of the continuously cast slab and deterioration of plastic deformation behavior.<sup>1)</sup> In hot direct rolling process, the as-cast  $\gamma$  grain structure acts as the initial microstructure for the subsequent thermo-mechanical treatment and entirely affects the size and morphology of the  $\alpha$ -ferrite and pearlite structure after A<sub>1</sub> transformation. Hence, the refinement of the as-cast  $\gamma$  grain structure is one of the most important issues in steel industries.<sup>2,3)</sup>

Recently, the present authors attempted to prevent the grain growth of the as-cast  $\gamma$  phase by pinning effect of TiB<sub>2</sub> particles.<sup>4)</sup> The titanium and boron with 1:2 molar ratio were added into S45C steel and the solidification structures in the sample cooled at 0.03°C/s were systematically investigated. It was shown that the additions of titanium and boron reduce the as-cast  $\gamma$  grain diameter down to a size of secondary Dendrite Arm Spacing (DAS) of  $\delta$  ferrite structure. However, the expected pinning particle, *i.e.*, TiB<sub>2</sub> was not found in the microstructure and, instead, there existed Ti(C,N) and Fe<sub>2</sub>B particles at the  $\gamma$  grain boundary which were considered to act as the pinning particles. This result is quite indicative of the possibility that the grain refinement of the as-cast  $\gamma$  grain structure can be realized by the addition of titanium only.

There have been a number of studies regarding the effect

of titanium addition on the microstructure of steels.<sup>5–8)</sup> The effect of titanium on fracture toughness in Heat Affected Zone (HAZ) of welded low carbon steels was investigated in the early works.<sup>5,6)</sup> It was shown that the titanium addition results in formation of titanium oxide which promotes the nucleation of ferrite inside the  $\gamma$  grain. Therefore, the titanium addition yields the grain refinement of ferrite structure in the HAZ, leading to improvement of the fracture toughness. Also, the titanium addition stabilizes titanium nitride at high temperatures and this nitride phase is quite effective in preventing the  $\gamma$  grain growth in the HAZ.<sup>7)</sup> Furthermore, the titanium addition retards the  $\gamma$  grain growth even during long time annealing processes between 900 and 1 250°C.<sup>8)</sup>

As mentioned above, the effect of titanium addition on the microstructure of the carbon steel is one of the issues widely addressed so far. However, little has been reported concerning its effect on the solidification structure of the carbon steel. In this study, we investigate the effects of the titanium addition on the solidification microstructure of S45C steel. The titanium addition dependences of as-cast  $\gamma$  grain size and the correlation between the  $\delta$  dendrite and  $\gamma$  grain structures are investigated in detail by a combination of slow cooling experiments and thermodynamic calculations.

## 2. Experimental Procedures

**Table 1** shows the chemical composition of the S45C steel rod with 20 mm diameter employed in this study. The

**Table 1.** Chemical composition of commercial S45C steel rod employed in this study (wt%).

C	N	Si	Mn	P	S	Al	O
0.45	0.0037	0.28	0.78	0.014	0.018	0.002	0.0114

sponge titanium of 99.5% purity was used as the additive material and our focus was placed on the range of titanium addition between 0 and 0.5 mol%, namely 0 to 0.435 wt%. In this paper, the titanium concentration is denoted in mol% to facilitate a comparison with the results obtained by titanium and boron additions in the previous paper.<sup>4)</sup> Phosphorous was also added to all the samples by 0.02 wt% to observe the  $\delta$  dendrite structure using the Oberhoffer's etching reagent. Kobayashi *et al.* reported that  $\gamma$  grain size of a low carbon steel decreases by half with a small amount of phosphorous addition (0.05 wt%).<sup>9)</sup> This refinement effect originates from the pinning effect of stabilized  $\delta$ -ferrite phase due to the phosphorous addition. It is considered that the refinement effect by phosphorous should occur also in the high carbon steel of our focus. However, the phosphorous concentration was taken to be same in all the samples. Therefore, the as-cast  $\gamma$  grain structure may be affected to the same degree by phosphorous addition in all the samples and it is allowed to discuss the effect of titanium only in the present results.

The sample of 130 g was put in an  $\text{Al}_2\text{O}_3$  crucible with an inner diameter of 35 mm and a depth of 45 mm and was melted at 1550°C in an SiC electric furnace filled with argon gas. The sample was held for 1 h at 1550°C, followed by cooling process at a rate of 0.03°C/s. The sample was quenched from 1100°C into strongly stirred iced water. The quenched sample was longitudinally sectioned and polished. The microstructural observation was performed by means of optical microscope and Scanning Electron Microscope (SEM) and the quantitative analysis was carried out by Energy Dispersive X-ray Spectrometry (EDS) and Electron Probe Micro-Analyzer (EPMA).

### 3. Results and Discussion

The as-cast  $\gamma$  grain structures with different amount of the titanium addition are shown in **Fig. 1**. It is seen that the increase in titanium addition leads to the reduction of  $\gamma$  grain size. The effect of titanium addition on  $\gamma$  grain diameter,  $d$ , is shown in **Fig. 2**. The structure without the titanium addition shows relatively coarse  $\gamma$  grains characterized by  $d=1.9$  mm. The addition of 0.1 mol% Ti reduces the  $\gamma$  grain size to about 0.5 mm and a further addition yields gradual decrement of the  $\gamma$  grain size, resulting in  $d=0.25$  mm in the sample with 0.5 mol% Ti. For comparison, the results with addition of titanium and boron with 1:2 ratio reported in the previous work<sup>4)</sup> are indicated by dashed line in **Fig. 2**. The grain size with the additions of titanium and boron is slightly smaller than the one with titanium only. This difference may originate from the formation of  $\text{Fe}_2\text{B}$  particle which was observed in the sample with titanium and boron.<sup>4)</sup> The grain sizes in both the cases are, however, almost the same. Therefore, it is considered that the grain refinement effect observed in the previous work<sup>4)</sup> should be ascribable mainly to the titanium addition.

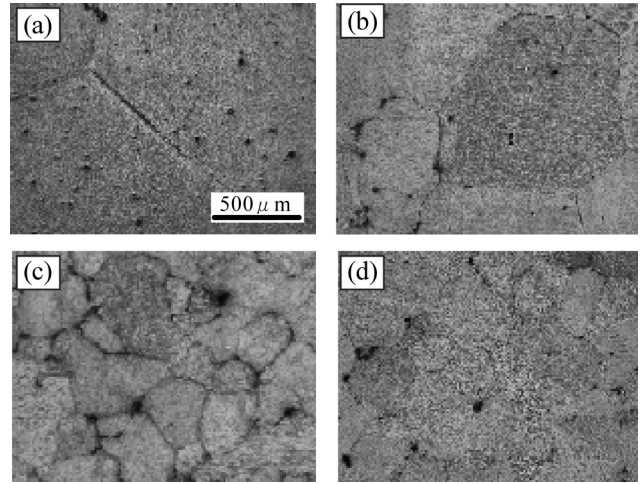


**Fig. 1.**  $\gamma$  grain structures (a) without Ti addition, (b) with addition of 0.05 mol% Ti, (c) with addition of 0.1 mol% Ti, and (d) with addition of 0.5 mol% Ti.

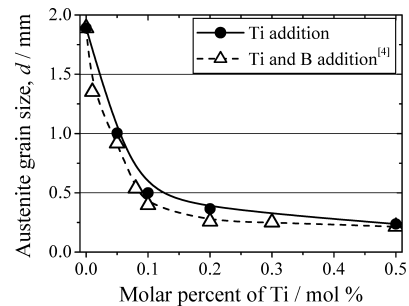


**Fig. 2.** Effects of Ti addition on  $\gamma$  grain size. The dashed line represents the results of Ti and B additions reported in the previous paper.<sup>4)</sup>

In **Fig. 2**, both the curves approach a certain small value. In the previous report,<sup>4)</sup> it was shown that this value corresponds to the secondary DAS. Hence, the correlation between the  $\gamma$  grain and dendrite structures was investigated in the present case, for the sample with titanium addition. **Figures 3(a)** and **3(b)** represent the  $\gamma$  grain and the dendrite structures, respectively, in the same region in the sample with 0.2 mol% Ti. In **Fig. 3(b)**, the dark region corresponds to the dendrite and the white line, which is drawn for visual aid, indicates the  $\gamma$  grain boundary. From these microstructures, it is comprehended that the  $\gamma$  grain boundary is located at the inter-dendritic position where the migration of the  $\gamma$  grain boundary is inhibited.

For further discussion, we calculate the phase diagram based on the CALPHAD approach, utilizing the thermodynamic database of the Fe–C–N–Ti quaternary system given by Lee.<sup>10)</sup> The calculated phase diagram for Fe–0.45wt%C–0.0037wt%N– $x$ Ti is shown in **Fig. 4** where the horizontal axis indicates the titanium concentration in mol%. This phase diagram shows that the Ti(C,N) is stabilized up to high temperatures by the titanium addition. In fact, as shown in **Fig. 5**, the particles were observed at the  $\gamma$  grain boundary and these were found to be Ti(C,N) by means of the EDS and EPMA analyses. In addition, there exist relatively large faceted particles of Ti(C,N) within the  $\gamma$  grain and at the  $\gamma$  grain boundary, as shown in **Fig. 6**. Hence, there are two type of Ti(C,N) particles observed in the sam-

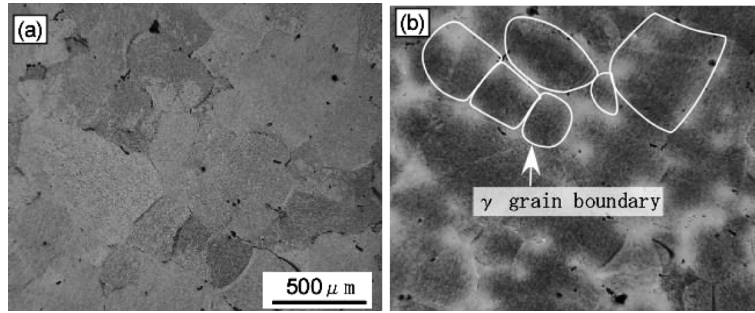


Fig. 3. Comparison between (a)  $\gamma$  grain and (b) dendrite structures at the same position in the sample with addition of 0.2 mol% Ti.

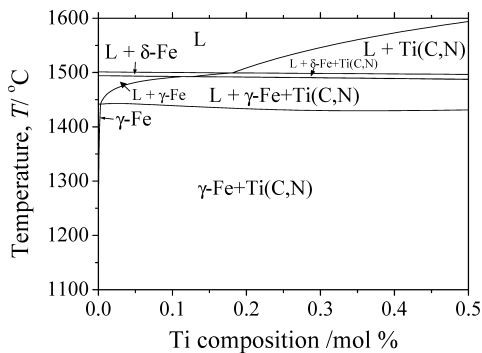


Fig. 4. Calculated phase diagram of Fe-0.45wt%C-0.0037wt%N-xTi steel.

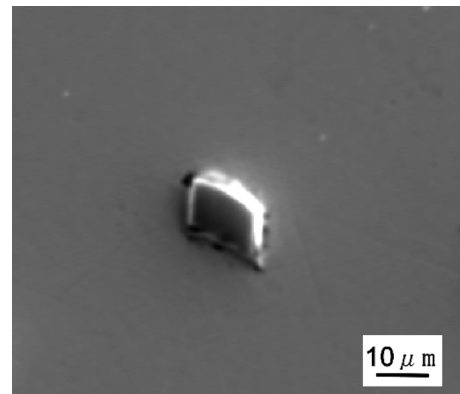


Fig. 6. SEM image of a large facet Ti(C,N) particle.

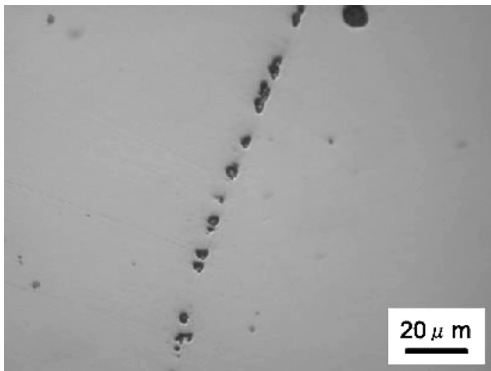


Fig. 5. Ti(C,N) particles existing at  $\gamma$  grain boundary.

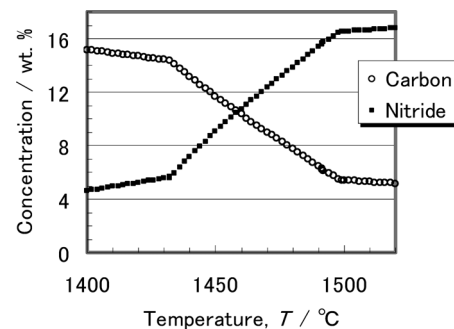


Fig. 7. Temperature dependence of C and N compositions in Ti(C,N) phase calculated by CALPHAD method for the sample with 0.45 wt% C, 0.0037 wt% N and 0.2 mol% Ti.

ple with the titanium addition, one is relatively small particles always locating on the  $\gamma$  grain boundary (Fig. 5) and the other is relatively large and faceted particles (Fig. 6) which is uniformly dispersed in the sample. The EPMA analysis revealed that the concentration ratio of nitrogen to carbon in these Ti(C,N) particles are different. The small Ti(C,N) particles contain a low concentration of nitrogen, while the large and faceted Ti(C,N) particles contain a high concentration of nitrogen up to about 38 at%. The temperature dependence of the carbon and nitrogen concentrations in Ti(C,N) phase was calculated and is shown in Fig. 7. The average concentration of titanium was set to be 0.2 mol%. As the temperature decreases, the concentration of nitrogen in Ti(C,N) decreases, while the concentration of carbon increases. Hence, it is considered that the small particle containing low concentration of nitrogen shown in Fig. 5 corresponds to the Ti(C,N) formed at low temperatures,

while the large and faceted particle with high concentration of nitrogen is the one crystallizing at high temperatures.

As discussed above, there are two types of Ti(C,N) particles. The pinning effect is considered to originate mainly from the small Ti(C,N) particles in the light of the fact that this type of particles were always found at the  $\gamma$  grain boundary. Furthermore, the migration of the  $\gamma$  grain boundary is inhibited at the inter-dendritic position. Hence, this type of pinning particles are considered to crystallize from the residual liquid at low temperatures, as is consistent with the above discussion regarding the nitrogen and carbon concentrations in Ti(C,N). In particular, from the phase diagram given in Fig. 4, this type of pinning particles are considered to form in L +  $\gamma$  + Ti(C,N) three phase region. This point is further addressed in the following.

It has been reported that in the hyperperitectic steel, the

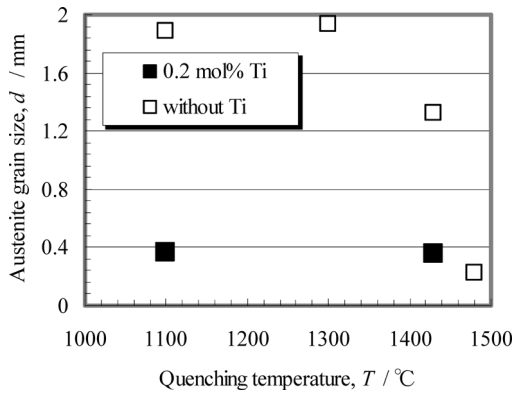


Fig. 8. Dependence of  $\gamma$  grain size on quenching temperature in the samples without Ti and with 0.2 mol% Ti.

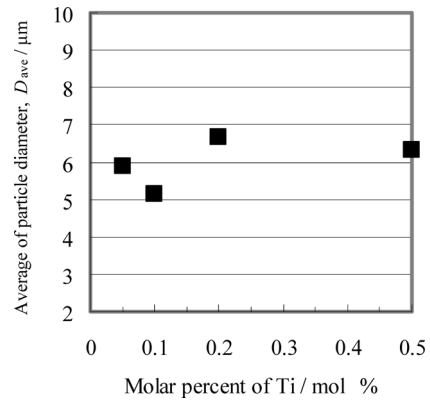


Fig. 9. Variation of Ti(C,N) particle size with respect to Ti composition.

liquid phase acts as a pinning phase for the  $\gamma$  grain growth in L+ $\gamma$  two phase region and the rapid  $\gamma$  grain growth occurs immediately after the solidification finishes.<sup>1)</sup> In order to clarify how the Ti(C,N) particles are involved in this grain growth process, the samples were quenched from the different temperatures during the cooling process at 0.03°C/s. The dependence of the  $\gamma$  grain diameter on the quenching temperature is shown in Fig. 8. In the sample without the titanium addition, the  $\gamma$  grain growth occurs drastically at high temperatures just after the liquid phase disappears ( $T \sim 1430^\circ\text{C}$ ). In contrast, the  $\gamma$  grains do not substantially grow at the high temperatures in the sample with 0.2 mol% Ti, and the grain size at 1100°C is almost the same as the one at 1430°C. Hence, the pinning effect by the titanium addition started at a temperature above the  $\gamma$ +Ti(C,N) two phase region. Also, the small Ti(C,N) particles were observed on the  $\gamma$  grain boundary in the sample with 0.2 mol% Ti quenched at 1430°C. Therefore, the Ti(C,N) pinning particles appear in the temperature region where the liquid phase still exists, more specifically, the pinning particles form in the L+ $\gamma$ +Ti(C,N) three phase region. This is consistent with the fact that the migration of the  $\gamma$  grain boundary is inhibited at the inter-dendritic position, indicating this type of pinning particles crystallize from the residual solidifying liquid. Furthermore, the comparison between the phase diagram of Fig. 4 and the results of Fig. 2 indicates that the  $\gamma$  grain diameter decreases with the increase in the crystallizing temperature of Ti(C,N) in L+ $\gamma$ +Ti(C,N) three phase region. The crystallizing temperature of Ti(C,N) in this three phase region is considered to be one of the important factors for refinement effect of the  $\gamma$  grain structure.

The grain refinement effect is discussed in terms of the size and the number of the Ti(C,N) particles. The average diameter of Ti(C,N) particles,  $D_{ave}$ , and the number of Ti(C,N) particles per unit area,  $n$ , were estimated based on the microstructural observation. The results of  $D_{ave}$  and  $n$  are plotted with respect to the amount of titanium addition in Figs. 9 and 10, respectively. As seen in Fig. 9, although the average diameter of Ti(C,N) particle seems to increase very slightly with the increase in the crystallizing temperature of Ti(C,N) (Fig. 4), all the values fall within a small range of 5–7  $\mu\text{m}$ . Figure 10 indicates that the number of Ti(C,N),  $n$ , significantly increases with the addition of titanium. Hence, the enhancement of the grain refinement effect

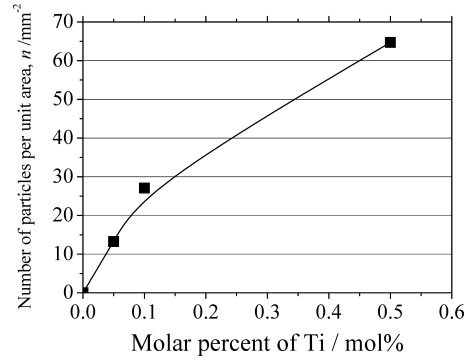


Fig. 10. Variation of the number of Ti(C,N) particles per unit area with respect to Ti composition.

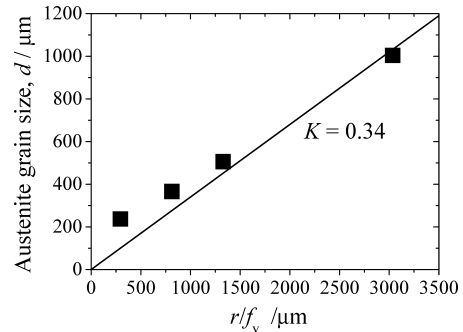


Fig. 11. Relation between  $r/f_v$  of Ti(C,N) and  $\gamma$  grain size.

due to Ti(C,N) results from the increment of the number of Ti(C,N) particles. The pinning effect is generally described by the following Zener equation,<sup>11)</sup>

$$d = K \frac{r}{f_v} \dots\dots\dots(1)$$

where  $d$  is the grain diameter,  $K$  is constant,  $r$  is the radius of pinning particle and  $f_v$  is the volume fraction of pinning particle. For the pinning phenomena due to carbide and nitride, the value of  $K=0.34$  yields quite reasonable agreement with the experimental data, especially, it has been reported that the pinning effect of Ti(C,N) on the  $\gamma$  grain growth can be well described with  $K=0.34$ .<sup>11)</sup> The relation between the  $\gamma$  grain size and  $r/f_v$  investigated in this study is shown in Fig. 11 in which the solid line represents the result of Eq. (1). One can see that the relation between  $d$

and  $r/f_v$  is approximately described by the Eq. (1). However, it is important to note the following point. The crystallization of Ti(C,N) occurs predominately in the inter-dendritic region where the solute elements are enriched due to the microsegregation during solidification. Accordingly, the distribution of Ti(C,N) particles is not spatially uniform so that the Ti(C,N) particles are dense at the inter-dendritic position while they are scarce inside the dendrite. In fact, it was observed in this study that the  $\gamma$  grain boundary is pinned at the inter-dendritic position. Therefore, in a strict sense, it may not be appropriate to discuss the pinning effect on the as-cast  $\gamma$  grain structure in the light of the Zener's relation which is based on the uniform distribution of the pinning particles. This is, in Fig. 11, realized from the fact that the experimental results deviate from Eq. (1) when the values of  $r/f_v$  are small. The small  $r/f_v$  value corresponds to the high titanium content and hence to the large number of Ti(C,N) particles nonuniformly distributed only in the inter-dendritic region. Namely, the deviation occurs when the distribution is strongly nonuniform. Moreover, the decrease in  $r/f_v$  value toward zero does not lead to decrease in measured grain size toward zero but toward 200  $\mu\text{m}$  which is close to the secondary DAS in the present sample. This is because the Ti(C,N) particles are distributed only in the inter-dendritic region. Yet, it would be worth stressing the fact that the pinning effect observed in this study can be approximately described by the relation of Eq. (1).

#### 4. Conclusions

The solidification experiments of S45C steel at a cooling rate of 0.03°C/s were carried out to investigate the effect of titanium addition on the as-cast  $\gamma$  grain structure. The important results are summarized as follows,

(1) The titanium addition leads to the refinement of as-cast  $\gamma$  grain size. The  $\gamma$  grain size is quite coarse,  $d=1.9$  mm, in the sample without the titanium addition and the  $\gamma$  grain size can be reduced down to about 0.5 mm by adding 0.1 mol% Ti. The further addition yields the gradual decrement of  $\gamma$  grain size.

(2) The  $\gamma$  grain size can be reduced to the size of the secondary DAS by adding more than 0.2 mol% Ti.

(3) Two types of Ti(C,N) particles exist in samples with the titanium addition; one is of small particle always locating on the  $\gamma$  grain boundary and the other is large and faceted particle uniformly dispersed over the sample. The thermodynamic calculation, EPMA analysis and microstructural observation indicate that the former type of particles crystallize in L+ $\gamma$ +Ti(C,N) three phase region and this type of particles play a dominant role in the grain refinement effect. Especially, the crystallizing temperature of Ti(C,N) in this three phase region is considered to be one of the important factors for refinement effect of the  $\gamma$  grain structure.

(4) The particle size of the Ti(C,N) does not depend substantially on the amount of titanium addition. The grain refinement effect due to Ti(C,N) is enhanced by the increment of the number of Ti(C,N) particles resulting from the titanium addition. Moreover, it was demonstrated that the relation between  $\gamma$  grain size, particle size and the volume fraction of Ti(C,N) can be approximately described by the Zener's relation.

#### REFERENCES

- 1) Y. Maehara, K. Yasumoto, Y. Sugitani and K. Gunji: *Trans. Iron Steel Inst. Jpn.*, **25** (1985), 1045.
- 2) N. Yoshida, Y. Kobayashi and K. Nagai: *Tetsu-to-Hagané*, **90** (2004), 198.
- 3) T. Maki: *Tetsu-to-Hagané*, **81** (1995), N547.
- 4) M. Sasaki, K. Matsuura and K. Ohsasa: *ISIJ Int.*, **48** (2008), 340.
- 5) K. Yokoyama, H. Ishikawa and M. Nagumo: *Tetsu-to-Hagané*, **83** (1997), 803.
- 6) K. Yamamoto, T. Hasegawa and J. Takamura: *Tetsu-to-Hagané*, **79** (1993), 1169.
- 7) S. Kanazawa, A. Nakajima, K. Okamoto and K. Kanaya: *Tetsu-to-Hagané*, **61** (1975), 2590.
- 8) H. Okaguchi and T. Hashimoto: *Tetsu-to-Hagané*, **72** (1986), S1385.
- 9) Y. Kobayashi, S. Iwasaki, K. Nakazato, T. Hibarui, S. Kuroda, N. Sakuma, N. Yoshida and K. Nagai: *ISIJ Int.*, **48** (2008), 344.
- 10) B.J. Lee: *Metall. Mater. Trans. A*, **32A** (2001), 2423.
- 11) P. A. Manohar, M. Ferry and T. Chandra: *ISIJ Int.*, **38** (1998), 913.